ACADEMIC PRESS

Available online at www.sciencedirect.com

SCIENCE DIRECT

Journal of Solid State Chemistry 171 (2003) 273–277

JOURNAL OF SOLID STATE CHEMISTRY

http://elsevier.com/locate/jssc

Optical study of $SrAl_{1.7}B_{0.3}O_4$:Eu, R (R = Nd, Dy) pigments with long-lasting phosphorescence for industrial uses

J. Sánchez-Benítez,[a] A. de Andrés,[a,*] M. Marchal,[b] E. Cordoncillo,[b] M. Vallet Regi,[c] and P. Escribano[b]

[a] *Instituto de Ciencia de Materiales de Madrid, Consejo Superior de Investigaciones Científicas, Cantoblanco, E-28049 Madrid, Spain*
[b] *Departamento de Química Inorgánica y Orgánica, Universitat Jaume I, E-12071 Castellón, Spain*
[c] *Departamento de Química Inorgánica y Bioinorgánica, Facultad de Farmacia, Universidad Complutense, E-28040 Madrid, Spain*

Received 6 May 2002; received in revised form 1 September 2002; accepted 6 September 2002

Abstract

We have studied and compared the optical properties of $SrAl_{1.7}B_{0.3}O_4$:Eu, R (R = Nd, Dy) pigments that present long-lasting phosphorescence obtained by different synthesis techniques. Samples obtained by ceramic methods, in our laboratories and by an industrial process, present better phosphorescent properties than those obtained by sol–gel technique. Raman spectra show that grinding produces severe damage of the lattice. We have obtained and analyzed the Eu^{3+} crystal field luminescence indicating that Eu^{3+} is found in quite different sites comparing ceramic and sol–gel samples. Codoping, with Nd or Dy is necessary in order to reduce the Eu^{3+} content, in all cases. The green luminescence band, obtained under UV illumination, can be fitted to two and three components in ceramic and sol–gel samples, respectively, due to different Eu^{2+} sites. Eu–Dy samples present the longest and the most efficient phosphorescence. The time evolution of the afterglow is well described by a t^{-1} law, up to about 2 h, indicating that the recombination process is achieved by electron–hole tunneling.

Keywords: Phosphors; Crystal field transitions; Raman phonons; Eu^{3+}; Aluminates

---

1. Introduction

Eu^{2+} activated phosphors MAl_2O_4 and $MAl_{12}O_{19}$ (M = Ba, Sr, Ca, Mg) are well known since the studies by Blasse et al. [1] in the 1960s. Their researches lead to the conclusion that these compounds were adequate phosphorescent materials because of their high quantum efficiency in the visible region. Phosphorescent properties of $SrAl_2O_4$:Eu^{2+} were studied by Palilla et al. [2], who determined that the green phosphorescent emission peaking at 520 nm was due to the $4f^65d \rightarrow 4f^7$ transition of Eu^{2+}. This parity-allowed transition has a quantum efficiency close to unity in a suitable crystalline environment. In the last decades, environmental considerations have motivated an increased demand for the development of radioactive-free luminous pigments, since the most handled ones use radioisotopes such as tritium (H-3) and promethium (Pm-147).

The long-lasting phosphorescence properties and the potential applications in optoelectronic devices [3,4] of $SrAl_2O_4$:Eu^{2+}–Dy^{3+}, $SrAl_2O_4$:Eu^{2+}–Nd^{3+} and $CaAl_2O_4$:Eu^{2+}–Nd^{3+} has renewed the interest in these compounds. Ito et al. [5] reported a reversible transition from monoclinic to hexagonal symmetry at 650°C in $SrAl_2O_4$. Some studies have concluded that only the monoclinic phase shows luminescent properties when doped with rare-earth ions. The transformation suffered by the samples with heat treatments makes industrial fabrication and tile production difficult.

Our objectives are basically the following: studying the best preparation method compatible with industrial processes, optimizing the phosphorescent properties and determining the best codopage conditions in order to increase the life time decay. Therefore, it is necessary to obtain, by industrial processes, powder samples with the best phosphorescent properties taking into account that during the posterior tile vitrification the phosphorescent pigments have to support thermal and grinding treatments.

---

*Corresponding author. Fax: +34-91-372-06-23.
E-mail address: ada@icmm.csic.es (A. de Andrés).

doi:10.1016/S0022-4596(02)00175-5

In the present work, we study the optical properties of samples obtained in our research laboratories and of the products obtained by industrial processes.

2. Experimental details

X-ray powder diffraction (XRD) was used in order to establish the homogeneity and purity of the fired samples in a Siemens D-5000 diffractometer with Cu $K\alpha 1$. Raman, luminescence and lifetime measurements were done in a home made Raman spectrometer with an Olympus microscope, a Jobin–Yvon monochromator and CCD. The samples were pressed into pellets except the industrial powder, where individual grains were studied. Optical measurements were also performed on the final tiles obtained from the industrial powder. All spectra were obtained at room temperature with a × 50 objective. Raman and luminescence spectra were obtained exciting with the 514.5 nm line of a Spectra Physics Ar–Kr laser and a Kaiser "Super-Notch Plus" filter to suppress the elastic light. Phosphorescence spectra were obtained with a white lamp and a filter that eliminated radiation above 340 nm.

Two synthesis methods, ceramic and sol–gel, were used to obtain phosphorescent pigments, both are compatible with industrial processes. Samples obtained with the conventional ceramic method, with nominal compositions, $Sr_{0.99}Eu_{0.01}RAl_{1.7}B_{0.3}O_4$ ($R = Dy_{0.02}$ or $Nd_{0.01}$), were prepared from stoichiometric amounts of $SrCO_3$, Al_2O_3, H_3BO_3, Eu_2O_3, Dy_2O_3 and Nd_2O_3. The mixture was ground and fired at 1200°C. In order to reduce the Eu (III) ions to Eu (II), the firing process was carried out in a tubular furnace with glucose. The raw powders were thermally treated up to 500°C in air atmosphere first and in nitrogen atmosphere at 1200°C for 1 h. Eu–Dy codoped compounds were also obtained by a ceramic method in an industrial environment. In this case three different types of grains larger than 50 μm were obtained.

The same compositions mentioned above were prepared by a sol–gel technique, consisting in a modified Pechini's method. The appropriate amount of $AlCl_3 \cdot 6H_2O$ was first dissolved in 25 mL of ethanol. In order to avoid the precipitation of $Al(ac)_3$, when the mixture of $Sr(ac)_2$ in ethanol is incorporated, 3 mL of H_2O (pH = 1) was added. After an homogeneous solution was attained, a suspension of $Sr(ac)_2$ in ethanol and an homogeneous solution of H_3BO_3 in ethanol were added with continued stirring. The mixture was refluxed at 80°C for two days. The gellification took place when citric acid was incorporated in a molar ratio citric acid:metal = 1:1. After 4 h, homogeneous and transparent gels were obtained. The resulting gels were dried at 80°C for two days and thermally treated. The green gels were fired in air at 1200°C/1 h. The organic material combustion of the gels gave a reducing atmosphere [6].

3. Results and discussion

We have firstly compared the samples obtained in our laboratories: ceramic and sol–gel methods. Two points are crucial: the reduction of Eu^{3+} to Eu^{2+} achieved by thermal treatments in a reducing atmosphere and the necessity to incorporate Boron in order to increase the fraction of monoclinic phase. The rare-earth doping of the present samples does not affect the formation of the phase of interest as checked by XRD [6].

Fig. 1 presents the luminescence spectra at RT under 514.5 nm excitation. Crystal field transitions of Eu^{3+} ions, $^5D_0$ to $^7F_{0,1,2}$, in sol–gel and ceramics samples are observed. Several peaks corresponding to the $^5D_0$ to $^7F_0$ transitions are detected indicating the presence of, at least, 2(3) sites for Eu^{3+} in sol–gel (ceramic) samples. The small differences in energy (about 15 cm^{-1}), in each kind of sample indicates very similar sites as expected considering the monoclinic crystallographic structure. Nevertheless strong differences can be easily observed between the two kind of samples (sol–gel and ceramic, Fig. 1). Therefore, Eu^{3+} have substantially different

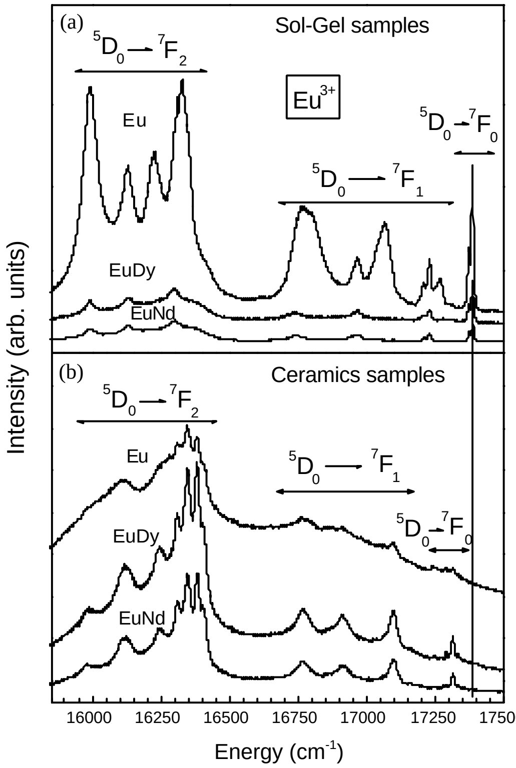

Fig. 1. Eu^{3+} luminescence spectra from $SrAl_{1.7}B_{0.3}O_4{:}Eu^{3+}R$ ($R = Nd^{3+}$, Dy^{3+}) made by both (a) sol–gel and (b) ceramics technique. $^5D_0 \rightarrow {}^7F_i$ ($i = 0, 1, 2$) transitions are indicated.

crystalline environments. This is probably due to the different proportion of the monoclinic phase in the compounds of each preparation method. The effect of codoping for both preparation methods is to reduce the Eu^{3+} content. The green phosphorescence intensity, under UV illumination, of the ceramic samples is higher than of the sol–gel ones. This is compatible to a higher proportion of monoclinic phase in the ceramic than in the sol–gel samples. Fig. 2 shows the different shape of the green phosphorescent band emission centered at 520 nm in both cases. This band can be fitted to 2 (512 and 547 nm) and 3 (506, 540 and 578 nm) Gaussian components in ceramic and sol–gel samples, respectively. Crystal field Eu^{3+} luminescence and Eu^{2+} phosphorescence are both indicating considerably different environments of these ions. Since the major phase detected by X-ray is monoclinic and Raman spectra show very similar lattice phonons it is possible that either the Eu ions are selectively doping the non-monoclinic phase, because of the sol–gel method, or that some Eu oxide is formed.

The samples obtained by industrial processes $SrAl_{1.7}B_{0.3}O_4$:Eu^{3+}–Dy^{3+}, results in three kinds of grains from 45 to 300 μm of diameter: white, yellow and black. As a result of a grinding process, all these components become a white fine powder (<45 μm). The Raman spectra obtained from the host (without doping), from different grains and from this resulting powder are shown in Fig. 3(a). White grain spectrum is very similar to the host spectrum while yellow grain shows only the strongest phonon at 465 cm^{-1}. This phonon is expected to correspond to the octahedral units (Al(Eu)–O_6) and can be considered as a molecular vibration. The other weaker peaks are lattice phonons where the long-range order determines their intensity and therefore are a measure of the lattice order. Black grain spectrum and ground powder shows a very low signal, no lattice peaks and an increase of the 465 cm^{-1} peak width. The lattices of these samples are severely damaged. In Fig. 3(b) Eu^{3+} crystal field luminescence of the mentioned samples are shown. Eu^{3+} is present in the white grains, but almost absent in yellow and black grains.

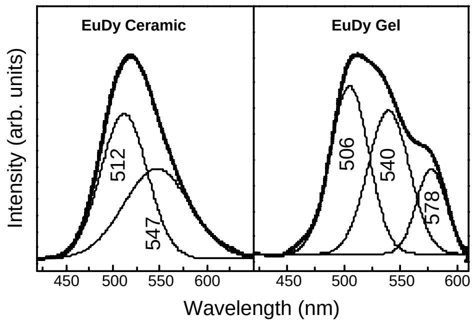

Fig. 2. Green phosphorescent emission band under UV illumination from (a) ceramic and (b) sol–gel samples, fitted by 2 and 3 bands, respectively.

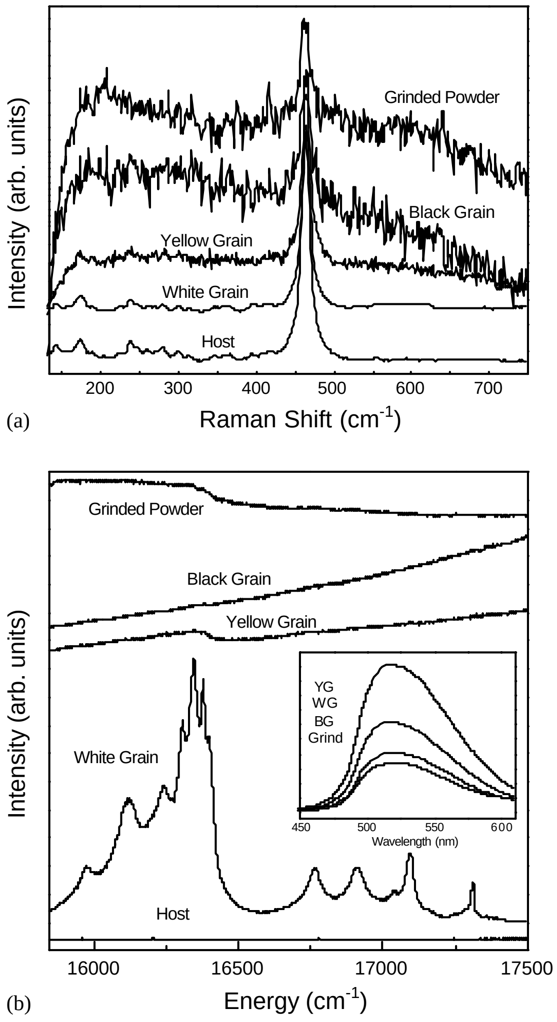

Fig. 3. (a) Raman spectra from host without doping, different industrial grains and final ground powder resulting from the previous ones (b) Eu^{3+} luminescence spectra from the same samples. Inset shows the green emission band from each type of grain and the grinded powder.

The 520 nm phosphorescent band for the different kinds of grains are similar to the ceramic samples (inset Fig. 3(b)). Yellow grains present the higher phosphorescent intensity and have been reduced almost completely, maintaining a good crystalline quality. It is noticeable that black grains and the ground powder have a good enough phosphorescent intensity, in spite of the fact that their lattices are considerably distorted.

Measurements of the evolution time of the afterglow have been carried out in the ceramic samples $SrAl_{1.7}B_{0.3}O_4$:Eu^{3+}, R^{3+} (Dy^{3+}, Nd^{3+}) for an afterglow time of 45 min. Note that in Fig. 4(a) the abscissa represents the time (min) in a reciprocal scale. The three samples accurately reproduce a behavior $I \sim t^{-1}$, with different slopes. Eu–Dy codoped sample has the longest and most efficient phosphorescence, followed by the Eu–Nd sample. Eu^{2+} ion is the emitter, while Nd^{3+} and Dy^{3+} ions operate as activator centers for the long-

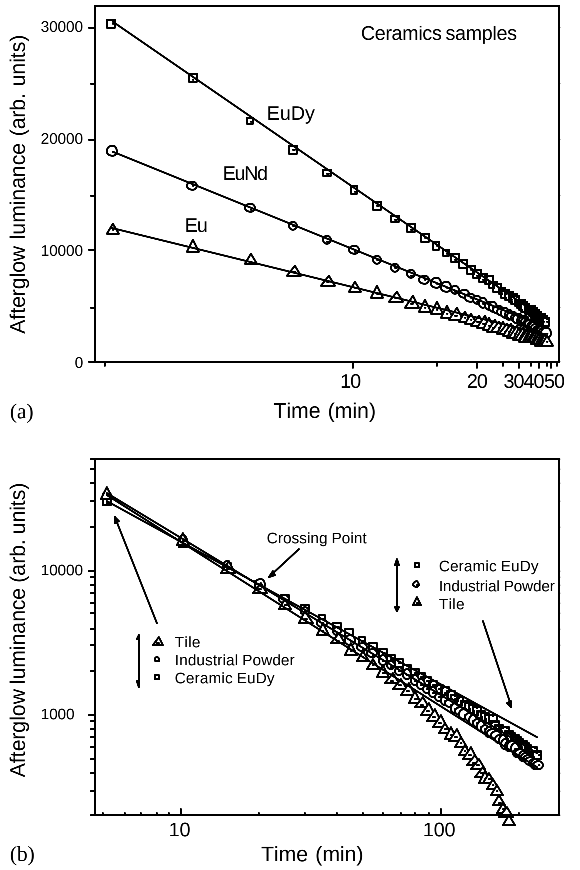

Fig. 4. Afterglow time evolution from (a) ceramic samples up to 45 min and (b) Eu–Dy codoped ceramic sample, industrial powder and final industrial tile up to 4 h.

lasting phosphorescence [3,4,7,8]. In the samples containing only Eu, Eu^{3+} ions are also acting as traps, but in this case the Eu^{2+} concentration is lower than in the codoped samples. High phosphorescence lifetime requires level traps to be located at an adequate depth according to the thermal release. The relative energy levels are determined by the lattice, in particular, by Eu^{2+} and R^{3+} environments. In case of having too deep trapping levels, the phosphorescence would not exhibit at room temperature; but if this trapping levels are too shallow, a fast decay will take place which will not last for long time. The optimum codopants concentration due to the solubility limit for 1% of Eu^{2+}, are 1% and 2% for Nd^{3+} and Dy^{3+}, respectively. Therefore a higher number of trapping levels in the Dy compound leads to a brighter phosphorescence.

Matsuzawa et al. [3] and by Jia et al. [8] proposed the energy level diagram of the $SrAlO_4$:Eu^{2+}–Dy^{3+} phosphor. Under UV illumination, an excited Eu^{2+} ion, can capture an electron from the valence band, becoming a metastable Eu^{+} state. The hole can migrate through the valence band and be captured by a trapping ion (Dy^{3+}, Nd^{3+} or non-reduced Eu^{3+}). This trapped hole will be released back to the valence band through thermal activation and recombined with the excess electron in the Eu^{+} ion. The relaxation of Eu^{2+} produces the green emission.

Hölsä et al. [9] proposed an alternative mechanism where the traps (oxygen and strontium vacancies) directly capture the excitation photons. The electron traps are then bleached thermally at room temperature and produce the electron–hole recombination process, which causes the excitation of the Eu^{2+} luminescence center by non-radiative energy transfer. The emission results from the normal de-excitation of the Eu^{2+} luminescence center.

Thermally stimulated recombination of trapped charge carriers results in a time dependence of the afterglow $I \sim t^{-a}$, with a close to 1. These kinetics are typical of recombination processes of electron–hole pairs through tunneling processes mediated by photo-carrier traps where the tunnel probability depends exponentially on the distance between the recombinating centers [10].

The time evolution of the phosphorescence intensity for long-lasting times (up to 4 h) for $SrAl_{1.7}B_{0.3}O_4$:Eu^{3+}–Dy^{3+} ceramic sample, the industrial grains and the vitrified tile from the industrial processes are shown in Fig. 4(b). All of them behave like $I \sim t^{-a}$, with a close to 1. Although, at short times, the Eu–Dy codoped ceramic sample shows the lower intensity, it exhibits the highest and longest phosphorescence intensity at long-lasting times. This is possible because of the different exponents a that allow the crossing, at about 20 min. The obtained exponent from the data fits, for times under 45 min, are: $a = 1.016$, 1.039, 1.116 for ceramic sample, industrial powder and tile, respectively, and $a = 1.117$, 1.179, 1.769 for the same samples at long-lasting time, between 45 min and 4 h.

4. Conclusions

We have studied the phosphorescent properties of $SrRAl_{1.7}B_{0.3}O_4$:$Eu_{0.01}$ ($R = Dy_{0.02}$, $Nd_{0.01}$) phosphors, obtained by two synthesis methods, ceramic and sol–gel. Crystal field transitions show that Eu^{3+} ions have substantially different crystalline environments in ceramic and sol–gel samples and that several sites are present for each sample. This can explain the differences in the green phosphorescence multicomponent bands. Phosphorescence intensity, under UV illumination, is higher in ceramic than in sol–gel samples. This is probably due to the different proportion of the monoclinic phase and of Eu^{2+}. The 520 nm band for the different kinds of industrial grains is similar to the ceramic samples one. The industrial grains present different reduction degrees of Eu^{3+}. The highest reduction corresponds to grains where the long-range order has almost disappeared while, surprisingly, maintaining a good enough afterglow intensity. Time evolution measurements show that afterglow luminance behavior is well described by a t^1 law, up to 2 h, showing that the recombination process takes place through electron–hole tunneling. Eu–Dy codoped samples show the most efficient and longest lasting phosphorescence in all cases.

References

[1] G. Blasse, A. Brill, Philips Res. Rep. 23 (1968) 201.

[2] P.C. Palilla, A.K. Levine, M.R. Tomkus, J. Electrochem. Soc.: Solid State Sci. 115 (1968) 642.

[3] T. Matsuzawa, Y. Aoki, N. Takeuchi, Y. Murayama, J. Electrochem. Soc. 143 (1996) 2670.

[4] H. Yamamoto, T. Matsuzawa, J. Lumin. 72–74 (1997) 287.

[5] S. Ito, S. Banno, K. Suzuki, M. Inagaki, Z. Phys. Chem. Neue Folge 105 (1977) 173.

[6] M. Marchal, M. Vallet-Regi, F. Conde, P. Escribano, J.B. Carda, E. Cordoncillo, J. Sánchez, A. de Andrés, J. Sol–Gel Sci. Technol., accepted for publication.

[7] V. Abbruscato, J. Electrochem. Soc. 118 (1971) 930.

[8] W. Jia, H. Yuan, L. Lu, H. Lin, W.M. Yen, J. Lumin. 76–77 (1998) 424.

[9] J. Hölsä, H. Jungner, M. Lastusaari, J. Niittykoski, J. Alloy Compds. 323–324 (2001) 326.

[10] C.J. Delbecq, Y. Toyozawa, P.H. Yuster, Phys. Rev. B 9 (1974) 4497.